Prediction-Correction Method for Optimization of Simulated Moving Bed Chromatography

Jason Bentley and Yoshiaki Kawajiri
School of Chemical and Biomolecular Engineering, Georgia Institute of Technology, Atlanta, GA 30332

DOI 10.1002/aic.13856
Published online June 15, 2012 in Wiley Online Library (wileyonlinelibrary.com).

A systematic algorithm for simulated moving bed (SMB) chromatography process development that utilizes dynamic optimization, transient experimental data, and parameter estimation to arrive at optimal operating conditions is described. These operating conditions ensure both high purity constraints and optimal productivity are satisfied. This algorithm proceeds until the SMB process is optimized without manual tuning. In a case study, it has been shown with a linear isotherm system that the optimal operating conditions can be reached in only two changes of operating conditions following the proposed algorithm. Another case study with a linear isotherm system has shown that the algorithm is robust to optimize the SMB even if there is significant model mismatch at first. © 2012 American Institute of Chemical Engineers *AIChE J,* 59: 736–746, 2013

Keywords: simulated moving bed, chromatography, process development, dynamic optimization, parameter estimation

Introduction

Simulated moving bed (SMB) chromatography is being utilized in an increasing number of applications in the life sciences including both small molecules such as sugars and enantiomers, and large molecules such as proteins. This is a simulated counter-current adsorption process which is discussed elsewhere.[1–3] For binary separations pure extract and raffinate products can be obtained with relatively high productivity and reduced solvent consumption compared to batch chromatography even if the separation factor is small. However, the determination of optimal operating conditions is not yet a straightforward task, especially if the sample volume available for lab and mini-plant tests is small or there is only a limited time for process design. Therefore, SMB is frequently applied using operating conditions that are known to be suboptimal in terms of productivity and solvent consumption.

The most commonly used SMB configuration for binary separations is to connect multiple chromatographic columns in series with the ability to switch the desorbent, extract, feed, and raffinate positions over time. A schematic of a 4-zone SMB configuration is shown in Figure 1. The feed is supplied between Zone 2 and 3 consisting of a mixture of species A and B, usually diluted in the desorbent D. The extract product is withdrawn between Zone 1 and 2 where the purity of B is high, and the raffinate product is withdrawn between Zone 3 and 4 where the purity of A is high. Desorbent is supplied between Zone 4 and 1 to regenerate the adsorbent. At the determined step time, the positions of the inlet/outlet ports switch ahead one column in the direction of fluid flow. This motion maintains the product purities in the extract and raffinate streams throughout the process.

Typical steps in SMB process design for a new separation problem are to perform batch experiments, find some operating conditions that are expected to satisfy purity constraints based on design criteria that approximate SMB dynamics,[4] then manually tune the operating conditions until the design specifications are met. Usually this effort is aided by mini-plant experiments and computer simulation of a process model.[5,6] And then there may be efforts to design more robust operating conditions where the separation performance is not adversely affected by slight disturbances in the flow rates, feed or desorbent compositions.

An important aspect of SMB process design is the selection of a process model and the determination of model parameters. Some detailed process models for chromatography have been developed[2] and there are a number of techniques that chromatographers have used for obtaining adsorption isotherm and kinetic parameters in the literature. Reviews of moment analysis of pulse injections, frontal analysis, elution by characteristic points, and inverse methods can be found.[2,3] Other researchers have studied ways to use batch experiments to estimate single-column model parameters to obtain a predictive process model for SMB. In Grosfils et al.[7] there is a comparison between different single-column models and a study of the identifiability of model parameters using pulse injections and parameter estimation. They used design of experiments to reduce the effort required to obtain reliable process model parameters for SMB. In Grosfils et al.[8] their SMB process model, which relies on careful descriptions of the extra-column dead volumes that exist in the real SMB unit, was validated by comparing it with SMB plant data. In Küpper et al.,[9] a concept for SMB model parameter estimation using online measurements is proposed and demonstrated using computational simulations of their

Correspondence concerning this article should be addressed to Y. Kawajiri at ykawajiri@chbe.gatech.edu.

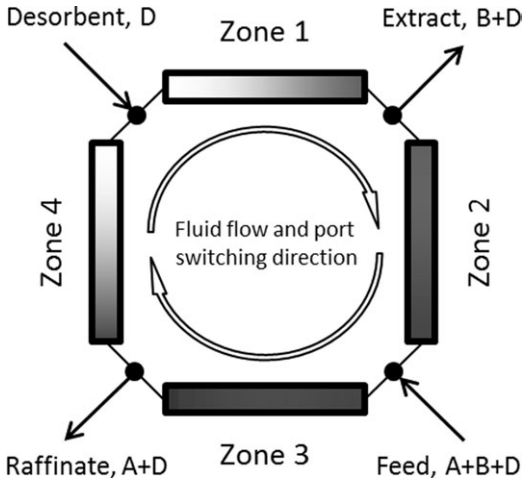

Figure 1. Schematic of 4-zone SMB with 4 chromatographic columns, 2 inlet streams and 2 outlet streams.

The mixture of species A and B is indicated by the darker shades in the columns. At the end of a step, the inlet/outlet ports switch to the adjacent port in the direction of fluid flow.

SMB plant model. They conclude that the model parameters can be estimated over time by transient measurements of the extract, raffinate and recycle lines and can be adapted to physical changes in the column properties such as the porosity. Yet their work requires online detection of entire internal concentration profiles over a step and no optimization is performed using the estimated parameters.

There are other researchers who have worked on automatic control of the SMB process using similar experimental measurements. In Klatt et al.,[10] a control strategy is described where the operating conditions and the assembled elution profile are measured during the periodic SMB operation and adjustments are made automatically to correct deviations from the desired product purities. Further work on optimizing control for SMB has been done at ETH Zurich in Grossmann et al.[11] where average product concentrations are measured during a cycle as feedback information for a controller. This measurement strategy also uses HPLC to analyze the product concentrations which is a more reliable measurement technique. Their methodology assumes that a reliable set of process model parameters and optimal operating conditions for the SMB are known *a priori*. They do not consider updating the SMB model parameters using the product concentration data.

The aim of this work is to demonstrate the prediction-correction algorithm for SMB process design starting from a new separation problem and ending with optimal operating conditions for the process. This algorithm uses a surrogate model (see Biegler et al.[12]), infrequent sampling of SMB outlet streams, parameter estimation, and dynamic optimization to reduce the time required to obtain reliable model parameters and optimize the SMB process in a systematic manner.

This article is organized as follows: The detailed steps of the prediction-correction algorithm are discussed in the Methodology section, our laboratory equipment is detailed in the Experimental section, and two case studies with a linear isotherm system are presented in the Results section to show that the algorithm converges efficiently and that the algorithm is robust to poor initial parameter values.

Methodology

Prediction-correction algorithm

The prediction-correction (PC) algorithm for SMB process development is outlined in Figure 2. This is an iterative scheme where in each iteration the SMB model parameters are corrected by fitting SMB experimental data and the optimal operating conditions are predicted by reoptimizing the SMB model using the refined parameter values. The algorithm is terminated when desired performance criteria are met.

This procedure assumes that a new mixture is to be resolved by SMB, and a reliable set of SMB model parameters is not yet known. The adsorbent, SMB column configuration, desorbent and feed compositions, and other operating parameters such as temperature should be selected first. The procedure is as follows:

1. Initialize $k = 0$. A set of batch experiments are performed on a single chromatographic column to estimate adsorption isotherm and kinetic parameters for a relatively simple SMB model.

2. Model-based optimization of the SMB operation is performed using nonlinear programming (NLP) to obtain an initial set of optimal operating conditions.

3. A SMB experiment is performed using the k^{th} optimal operating conditions and a set of concentration data and product purities are obtained.

4. Let $k = k + 1$. The adsorption isotherm and kinetic parameters are refined by a least-squares parameter

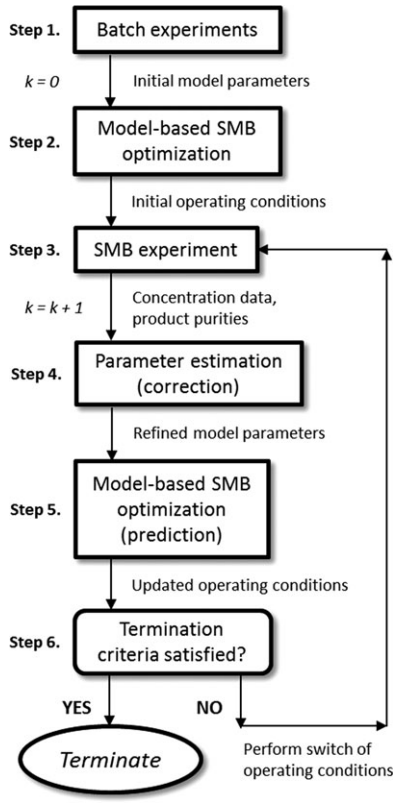

Figure 2. Prediction-correction (PC) algorithm for SMB process development.

estimation comparing the SMB model to the experimental concentration data (correction step).

5. Model-based optimization of the SMB operation is repeated with the refined set of model parameters to obtain an updated set of optimal operating conditions (prediction step).

6. The termination criteria are checked: if the product purity constraints were met by the k^{th} SMB experiment and the $k + 1^{th}$ optimal throughput is not significantly different from the k^{th} optimal throughput, then the algorithm is terminated. If not, then return to Step 3 and repeat.

Step 1: Batch Experiments

The SMB model considers individual chromatographic columns, column connections, and inlet/outlet streams. The chromatographic column model consists of component mass balances in the liquid and stationary phases, adsorption isotherm relations, and mass transfer/diffusion relations where the only unknown parameters are the adsorption isotherm and kinetic constants. There are more sophisticated models that could be used to include model parameter dependencies on flow rate, such as the van Deemter relation[3] showing the effect of flow rate on mass-transfer coefficients. Furthermore, more detailed column models that consider the dead volume can be found in the literature.[13]

In this work, we assume a linear isotherm and the linear driving force (LDF) model in the stationary phase, so there is one equilibrium constant (Henry's constant) and one overall mass-transfer coefficient to be determined for each adsorbing species in the system. For binary separations, this corresponds to four model parameters [see (2) and (3)]. Hence, the following batch experiments and calculations are needed:

1. Small volume pulse injection of tracer compound to estimate the overall porosity of the column.

2. Small volume pulse injection of feed mixture to estimate the Henry's constants and mass-transfer coefficients by retention times and the number of theoretical plates (NTP) for each species.

The Henry's constant for a given compound is a function of the column porosity, and the estimate of the mass-transfer coefficient is a function of the column porosity, plate number and flow rate. However, these batch experiments yield a set of initial model parameters that are not measured at various conditions, and they do not account for any dead volumes or mixing behaviors in the real SMB unit. In our approach, we do not need such models that require extra experimental effort. These initial parameter estimates are used only to obtain an initial set of optimal operating conditions which are later corrected iteratively.

Mathematical modeling of SMB

The SMB model used in this work resembles closely the kinetic model used in Grosfils et al.[8] and the SMB optimization problem formulation is the same as the single-step formulation implemented in Kawajiri and Biegler.[14] In the next subsections, the details of the SMB model and NLP problem are discussed.

For each column, the component mass balance in the liquid phase is stated as

$$\frac{\partial c_i^j(z,t)}{\partial t} + \frac{1-\varepsilon_b}{\varepsilon_b}\frac{\partial q_i^j(z,t)}{\partial t} = -v^j(t)\frac{\partial c_i^j(z,t)}{\partial z} \qquad i = A,B \quad j = 1,2,\ldots,n_{\text{col}} \tag{1}$$

where c_i^j is the liquid phase concentration of component i in column j, ε_b is the overall bed porosity, q_i^j is the adsorbed phase concentration of component i in column j, v^j is the linear mobile phase velocity in column j, z is the axial coordinate, t is the time, alphabetic characters are used according to the number of adsorbable components in the system ($i = A$, B for binary separation), and n_{col} is the number of columns.

The LDF mass transfer relation is given as

$$\frac{\partial q_i^j(z,t)}{\partial t} = k_i\left(q_i^{\text{eq},j}(z,t) - q_i^j(z,t)\right) \tag{2}$$

where k_i is the overall mass-transfer coefficient for component i, and $q_i^{\text{eq},j}$ is the adsorbed phase concentration of component i in equilibrium with the liquid phase in column j. This model assumes that the primary resistance to mass transfer exists in the adsorbed phase. In the LDF model, k_i is a lumped parameter used to describe band broadening effects.[3]

The linear isotherm is stated as

$$q_i^{\text{eq},j}(z,t) = H_i c_i^j(z,t) \tag{3}$$

where H_i is the Henry's constant for component i.

The boundary conditions for (1) are

$$c_i^j(0,t)v^j(t) = c_{i,\text{in}}^j(t)v_{\text{in}}^j(t) + \gamma_f^j(t)c_{i,f}v_f \tag{4}$$

where $c_i^j(0,t)$ is the concentration of component i in column j at position $z = 0$, the column entrance, $c_{i,\text{in}}^j$ is the concentration of component i in the inlet connection to column j, v_{in}^j is the velocity in the inlet connection to column j, γ_f^j is a binary variable equal to 1 if column j is at the feed location and 0 otherwise, $c_{i,f}$ is the concentration of component i in the feed, and v_f is the feed velocity. Because only one column is at the feed location at a time, $\gamma_f^j = 0$ for all columns but one during a given step of the SMB process.

To model the inlet/outlet ports, overall mass balances are used which reduce to the following equations

$$\begin{aligned} v^j(t) &= v_{in}^j(t) + \gamma_d^j(t)v_d + \gamma_f^j(t)v_f \\ v_{\text{out}}^j(t) &= v^j(t) - \gamma_e^j(t)v_e - \gamma_r^j(t)v_r \end{aligned} \tag{5}$$

where γ_d^j is a binary variable for the desorbent location, v_d is the desorbent velocity, v_{out}^j is the velocity in the outlet connection of column j, γ_e^j is a binary variable for the extract location, v_e is the extract velocity, γ_r^j is a binary variable for the raffinate location, and v_r is the raffinate velocity. The binary variables equal 1 if column j is at the inlet/outlet location and 0 otherwise. These equations assume constant cross-sectional areas in the columns and connections so that conversions from volumetric flow rates to velocites in the tubing are not necessary.

To model column connections the following equations are used

$$\begin{aligned} c_{i,\text{in}}^j(t) &= c_{i,\text{out}}^{j-1}(t), \quad j = 2,3,\ldots,n_{\text{col}} \\ c_{i,\text{in}}^1(t) &= c_{i,\text{out}}^{n\text{col}}(t) \\ v_{\text{in}}^j(t) &= v_{\text{out}}^{j-1}(t), \quad j = 2,3,\ldots,n_{\text{col}} \\ v_{\text{in}}^1(t) &= v_{\text{out}}^{n\text{col}}(t) \end{aligned} \tag{6}$$

where $c_{i,\text{out}}^j$ is the concentration of component i in the outlet connection of column j. We also use the simple relation

$$c^j_{i,\text{out}}(t) = c^j_i(L_c, t) \tag{7}$$

where $c^j_i(L_c, t)$ is the concentration of component i in column j at position $z = L_c$, and L_c is the column length.

Numerical simulation of the SMB model

In the SMB model, (1) and (2) are discretized in the axial coordinate so that these partial differential equations are reduced to a system of ordinary differential equations. The discretization is done in gPROMS using a second-order central finite difference method with 100 finite elements in the axial domain of each column. The resulting system of differential algebraic equations (DAEs) consisting of (1)–(7) are solved by the method of lines[15] with initial conditions specified for the concentration of each component at each axial position in both liquid and adsorbed phases. For a simulation starting from clean beds the initial conditions are $c^j_i(z, 0) = 0$ and $q^j_i(z, 0) = 0$ for all $i = A, B$ and all $j = 1,2,\ldots,n\text{col}$ and all $z = (0, L_c]$.

Steps 2 and 5: Model-Based SMB Optimization (Prediction Step)

The following model-based SMB optimization is performed initially in Step 2 of the PC algorithm as shown in Figure 2 and then again in Step 5 of each iteration. In this work, the SMB optimization objective function $\phi_{\text{SMB}}(u)$ is stated as maximization of the feed flow rate F_f, which is a measure of productivity. The optimization problem is formulated as

$$\max \quad \phi_{\text{SMB}}(u) = F_f \tag{8}$$

$$\begin{aligned} \text{s.t.} \quad & \text{Purity}^r_A \geq \text{Purity}^r_{A,\min} \\ & \text{Purity}^e_B \geq \text{Purity}^e_{B,\min} \end{aligned} \tag{9}$$

$$\begin{aligned} c^j_i(z,0) &= c^{j+1}_i(z, t_S), \quad j = 1, 2, \ldots, n\text{col} - 1 \\ c^{n\text{col}}_i(z,0) &= c^1_i(z, t_S) \\ q^j_i(z,0) &= q^{j+1}_i(z, t_S), \quad j = 1, 2, \ldots, n\text{col} - 1 \\ q^{n\text{col}}_i(z,0) &= q^1_i(z, t_S) \end{aligned} \tag{10}$$

$$\begin{aligned} & F^k \leq F_{\max}, \quad k = 1, 2, 3, 4 \\ & \text{Equations (1)–(7)} \end{aligned} \tag{11}$$

where u is the control vector of SMB operating conditions $u^T = [m^1, m^2, m^3, m^4, t_S]$, t_S is the step time, m^k is the liquid to solid flow rate ratio in zone k, which is given as

$$m^k = \frac{F^k t_S - V_c \epsilon_b}{V_c(1 - \epsilon_b)} \tag{12}$$

where F^k is the volumetric flow rate in zone k, and V_c is the total column volume. With these m-values specified, the optimal flow rates can be calculated given the column volume and overall porosity. The purity constraints in (9) require that the purity of component A in the raffinate must be at least the minimum required and the purity of component B in the extract must be at least the minimum required. Components A and B are the less and more retained components respectively. The cyclic steady state (CSS) constraints in (10) are defined for a single step of the SMB process. This problem formulation was first proposed for periodic adsorption processes by Nilchan and Pantelides,[16] and was implemented for SMB optimization in Kawajiri and Biegler.[14] The CSS constraints mean that the liquid and adsorbed phase concentration profiles are the same at the beginning and end of a step only shifted one column in the direction of fluid flow. The maximum flow rate constraints in (11) are based on the total pressure drop limits for the SMB pumps.

It should be noted that the PC algorithm is designed for finding the optimal operating conditions and reliable parameter values at the process development stage for a new separation problem. In contrast, rejecting disturbances and dealing with unexpected changes in physical properties during continuous operation (pump flow rates, void ratio, etc.) are out of scope of this article. To correct the operating conditions in a timely manner for such time-varying changes, an optimal control problem that takes into account the entire transient profile, not a CSS optimization problem, must be solved online. In addition, a reliable state estimation technique would enable fast and effective control actions.[10,11] For such problems, employing efficient and reliable computational methods for online calculations is crucial.

Numerical optimization

The SMB optimization problem (8)–(11) is formulated as a NLP problem and solved by the SRQPD solver in gPROMS. The solution method requires the time integration of the DAE system (1)–(7) for a single step using the method described in the numerical simulation section. The Karush-Kuhn-Tucker system is obtained by evaluating sensitivity equations during the time integration of the DAE system. The size of the NLP scales with the number of columns in the SMB and the number of axial discretization points in each column. To initialize the NLP, a guess for the CSS concentration profiles must be provided, and the CSS constraints are checked at the end of integrating the DAE system in each iteration of the optimization algorithm. For initialization of the NLP in Step 2 of the PC algorithm, the operating conditions are selected so that the triangle theory constraints set forth in Mazzotti et al.[4] are satisfied, but these constraints are not needed in subsequent iterations.

Step 3: SMB Experiment

The SMB experiment involves switching to the current optimal operating conditions and then measuring transient concentration data from the extract, raffinate and recycle lines. Numerous sampling strategies are feasible. One such sampling strategy, which is employed in our case studies, is as follows: At the moment the operating conditions are switched, the product streams (extract and raffinate, see Figure 3) are fed into empty containers and the cumulative product is collected. At the end of a number of steps a small sample is taken from the product containers and its composition is analyzed by HPLC. This generates a set of concentration data for each product line over time.

For each SMB experiment the product samples are collected at the end of a number of steps until the change in the measured concentration in the n^{th} sample is sufficiently small. For each sample in the k^{th} experiment, the following condition is checked

$$\left| \frac{\sum_{i=A,B} c^e_i(n-1) - \sum_{i=A,B} c^e_i(n)}{\sum_{i=A,B} c^e_i(n-1)} \right| \leq \epsilon^k_c \tag{13}$$

where $c^e_i(n)$ is the concentration of component i in extract sample n, and ε^k_c is the tolerance for the change in concentration of the extract product in the k^{th} experiment. If the inequality (13) is satisfied for sample n, then no more sampling needs to be done, and the experiment can be

terminated. Condition (13) is checked only for the extract samples since the strongly adsorbed component requires a longer time to reach the CSS.

There may be significant contaminations in the product streams as well as significant concentrations in the recycle loop. To increase observability of the process, we sample the recycle stream over a single step to obtain average concentrations, as shown in Figure 3, after the sampling of extract and raffinate products is finished. It should be noted that more frequent sampling from the recycle line may further increase the observability. However, this was not done in our study.

Step 4: Parameter Estimation (Correction Step)

The parameter estimation is formulated as a maximum likelihood problem in gPROMS[17] where the objective function is

$$\phi_{\mathrm{PE}}(\theta) = \sum_{p=1}^{\mathrm{NE}} \sum_{l=1}^{\mathrm{NV}_p} \sum_{n=1}^{\mathrm{NM}_{pl}} \left[ln(\sigma_{pln}^2) + \frac{(\tilde{z}_{pln} - z_{pln})^2}{\sigma_{pln}^2} \right] \tag{14}$$

where θ is the set of model parameters to be estimated, NE is the number of experiments, NV_p is the number of variables measured in the p^{th} experiment, NM_{pl} is the number of measurements of the l^{th} variable in the p^{th} experiment, σ_{pln}^2 is the variance of the n^{th} measurement of the l^{th} variable in the p^{th} experiment, which is determined by the measured variable's variance model, $\tilde{z}_{pln}$ is the n^{th} measured value of the l^{th} variable in the p^{th} experiment, and z_{pln} is the n^{th} model-predicted value of the l^{th} variable in the p^{th} experiment. The measured variables are the concentration data obtained from the SMB experiment(s), and the model-predicted variables are the concentration values calculated by numerical integration of the SMB model (1)–(7).

The parameter estimation problem is formulated as

$$\min \quad \phi_{\mathrm{PE}}(\theta) \tag{15}$$

$$\begin{aligned} &\text{s.t.} \quad \theta_{\min} \le \theta \le \theta_{\max} \\ &\text{Equations (1)–(7)} \end{aligned} \tag{16}$$

where $\theta_{\min}$ and $\theta_{\max}$ are the lower and upper bounds on the set of model parameters to be estimated. The bounds on θ are used to avoid unreasonable changes in the parameter values, and we confirm that they are not active at the optimal solutions.

The SMB parameter estimation problem (15) was solved by the SRQPD solver in gPROMS. This is the same dynamic optimization solver that was used for the NLP problem (8) in Steps 2 and 5. The computation time of the parameter estimation problem was found to scale with the number of SMB experiments that were simulated.

The parameter estimation routine in gPROMS also includes statistical analysis of the estimated parameters. The statistics of interest are the confidence intervals for the estimated parameters. These values represent bounds on the estimated parameters where 95% of the observed data is described by parameter values within the intervals under some assumptions. The details of this calculation can be found in the gPROMS documentation.[17]

An important element of the maximum likelihood objective function (14) and the confidence interval calculation is the variance model definition, σ_{pln}^2 for the experimental measurements. A variance model can be obtained for the concentrations measured by HPLC using calibration curve data. The calibration curve for each component may consist of three or more data points for each concentration level. From this data the deviation of each measured concentration from that predicted by the regression model used in the calibration curve can be calculated. Here, the variance σ_{pln}^2 may be dependent on the measured value z_{pln}. In this work, we use a linear variance model depending on the measured concentration as

$$\sigma_{pln}^2 = (\alpha z_{pln} + \beta)^2 \tag{17}$$

where α and β are regression coefficients fit to the standard deviations calculated at each concentration level in the calibration curve. We assume that the linear variance model describes the positive correlation between concentration and variance. And a linear variance model with positive slope ($\alpha > 0$) lends additional weight to those experimental data points with low concentrations in the parameter estimation, since the smaller the variance of a measurement the greater the corresponding multiplier in the objective function (14).

Step 6: Termination Criteria

An important aspect of the PC algorithm is that it has systematic termination criteria. We use the following two criteria that must both be satisfied before termination of the PC algorithm occurs. The termination criteria we used are:

1. The purity constraints (9) are satisfied in the k^{th} SMB experiment.

2. In the $k + 1^{th}$ SMB optimization problem the optimal objective value, $\phi_{\mathrm{SMB}}(u_{k+1})$ should not differ significantly from the previous optimal objective value $\phi_{\mathrm{SMB}}(u_k)$. The following condition should be satisfied

$$\left| \frac{\phi_{\mathrm{SMB}}(u_k) - \phi_{\mathrm{SMB}}(u_{k+1})}{\phi_{\mathrm{SMB}}(u_k)} \right| \le \epsilon_{\mathrm{tol}} \tag{18}$$

where $\varepsilon_{\mathrm{tol}}$ is the tolerance set for the change in the objective function between successive SMB optimization problems.

If both of the above conditions are satisfied then the $k + 1^{th}$ SMB experiment is deemed to be unnecessary. Thus, the PC algorithm is terminated and the current operating conditions in the k^{th} experiment, u_k are considered optimal.

Experimental

SMB equipment and test system

The experiments were performed using a laboratory scale SMB unit (CSEP C190, Knauer, Berlin, Germany). A schematic of the SMB unit is shown in Figure 3 to illustrate the columns connected to a rotary valve and the sampling locations. The unit includes four double-piston pumps (P1 through P4), two ultra-violet detectors at the extract and raffinate outlet streams, and a rotary valve with 16 positions. The ports of the rotary valve are connected to each other by continuous channels. All unoccupied positions were filled with short capillary tubing. Four HPLC columns (YMC-Pack ODS-A, YMC, Japan), labeled (C1–C4) were employed in a 4-zone configuration with one column in each zone (1-1-1-1). The HPLC column dimensions are 250 mm length and 10 mm inner diameter. They are packed with a C18 stationary phase for reverse phase chromatography with an average particle size of 20 μm.

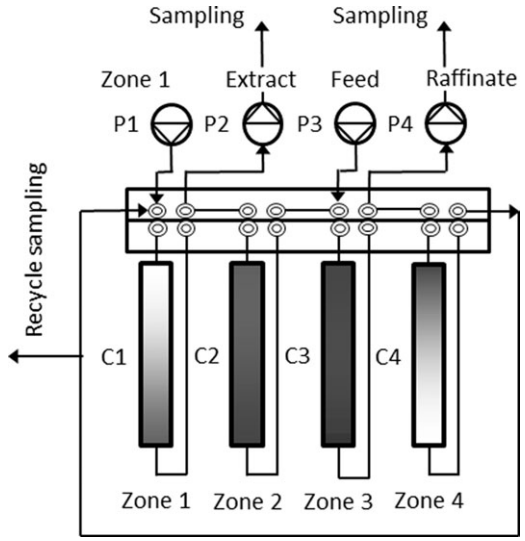

Figure 3. Schematic of SMB unit with four pumps (P1 through P4), and sampling points at the extract, raffinate and recycle lines.

Four HPLC columns (C1 through C4) are in a 4-zone 1-1-1-1 configuration.

SMB experimental technique

During an SMB experiment the extract and raffinate lines were placed in clean glass containers with magnetic stirring so that the cumulative products were collected. The sampling technique was described in section Step 3 on the SMB experiment. The composition of each sample was analyzed by a Shimadzu analytical HPLC with the following components: LCsolution version 1.24 SP1 controlling software, and an analytical C18 column (Daisopak, SP-120-10-ODS-BP, Daiso, Japan). Also, the average pump flow rates were measured periodically using a flowmeter (Model 5025000, GJC Instruments) at the extract outlet, raffinate outlet, and recycle line between Zone 4 and Zone 1 (referring to Figure 3) during each experiment to verify the operating conditions. The UV signals at the extract and raffinate points were monitored, but this data was not used in the parameter estimation because of poor baseline quality and the need for deconvolution of the signal.[11] In addition, the average extract and raffinate product concentrations were sampled for an entire step after the first set of samples were taken and the product purities were checked against the purity constraints (9).

Determination of variance model for parameter estimation

Using the Shimadzu HPLC unit and the analytical C18 column, calibration curve data for uridine and guanosine were obtained. Uridine (CAS 58-96-8, EMD Biosciences) and guanosine (CAS 118-00-3, Spectrum Chemical Mfg.) were injected as one-to-one mixtures dissolved in 85% water 15% methanol. These data and the standard deviations at each concentration level for uridine and guanosine are shown in Figure 4.

We perform a linear regression on the standard deviation data to obtain the coefficients in the linear variance model (17). The coefficients $\alpha = 0.0045$, $\beta = 0.23$ are the average slope and intercept values for uridine and guanosine from the standard deviation data in Figure 4. Because we observed that the variance has a slight positive correlation with concentration, a linear variance model is the most simple way to quantify this relationship. We observed an increase in σ^2_{pln} for both uridine and guaosine as concentration increases, but a notable difference in σ^2_{pln} for uridine and guanosine was not found at any concentration level. We believe the observed variances are probably due to errors in the injection volume for repeated injections and perhaps also errors in baseline determination during the calculation of chromatogram peak areas.

Results

Convergence of proposed algorithm

We demonstrate that the PC algorithm converges efficiently so that only a few changes of SMB operating conditions are needed to reach the purity constraints with optimal productivity. The initial parameter set, θ_0 was obtained by batch experiments on a single HPLC column, which was one out of four used in the SMB unit. The desorbent was 90% water 10% methanol. The feed was 39 mg L^{-1} uridine and 39 mg L^{-1} guanosine dissolved in the desorbent. The overall porosity of the column was calculated to be $\varepsilon = 0.820$ by measuring the retention time of uracil, which is often used in reversed phase chromatography to measure the porosity. Nevertheless, we observe a small change when the desorbent

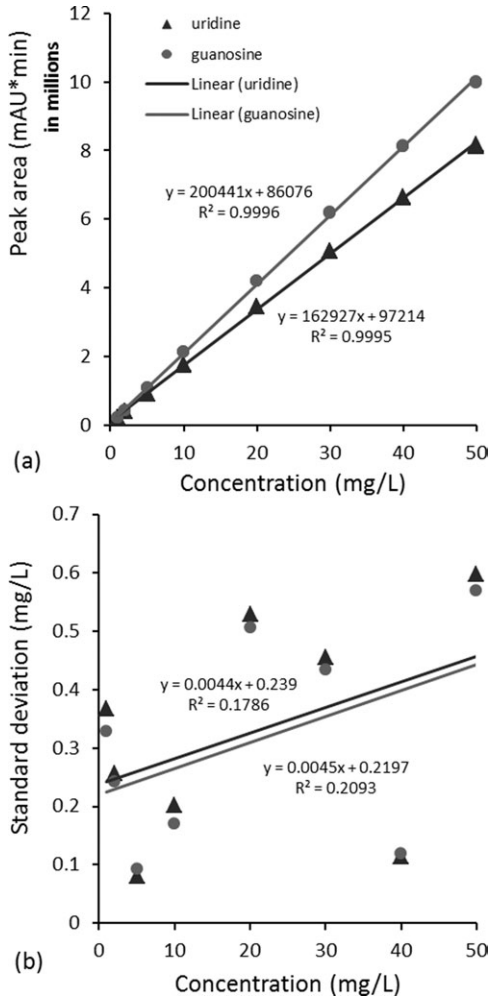

Figure 4. (a) Calibration curve using Shimadzu HPLC with three injections made at each concentration level; (b) standard deviations of the measured concentration at each concentration level, the regression equations and coefficients are included.

Table 1. Refinement of θ_k by Parameter Estimation

Parameter	θ_0	θ_1	θ_2	θ_3
H_A	0.846	1.00	0.983	0.971
H_B	2.75	2.82	2.84	2.80
k_A, min^{-1}	103	52	90	52
k_B, min^{-1}	161	81	58	81

composition is changed, and we update the value of ε for different desorbent composition. The Henry's constants, H_i for uridine (A) and guanosine (B) were calculated by measuring the retention times of uridine and guanosine after a 30 μL pulse injection of the SMB feed mixture, and the mass-transfer coefficients, k_i were calculated by measuring also the peak width at half peak height for uridine and guanosine using the same pulse injection. This parameter set, θ_k was refined by parameter estimation after each SMB experiment. The initial parameter set and each parameter estimation solution are shown in Table 1.

The SMB optimization problem (8)-(11) was solved in the kth iteration using θ_k with the purity constraints $\text{Purity}_A^r \geq 96\%$ and $\text{Purity}_B^e \geq 96\%$, and with $F_{\max} = 10$ mL min^{-1}. The objective function convergence tolerance, ε_{tol} in (18) was set to 0.05. The optimal operating conditions, u_k are predicted to satisfy the purity constraints at maximum throughput. These conditions were implemented in the kth SMB experiment until the PC algorithm termination criteria were met. The optimal operating conditions are shown in Table 2 along with the experimental product purities obtained in the kth experiment and the normalized change in throughput from (18). In all optimal solutions the Zone 1 flow rate F^1 reached the upper bound of 10 mL min^{-1} so that larger concentrations of components can be sufficiently desorbed when the feed flow rate is maximized.

In this case study, we found that the PC algorithm required only three iterations for the termination criteria to be met. This corresponds to only two changes of the SMB operating conditions from the initial guess. It is clear from Table 2 that the product purity constraints were violated in SMB experiments 1 and 2. The SMB experimental data for $k = 0$–2 are displayed together in Figure 5. The termination criteria were satisfied at $k = 2$ because the product purities in SMB experiment 3 were both over 96% and (18) was satisfied. Because the termination criteria were satisfied at $k = 2$, the optimal operating conditions u_3 were not used, and u_2^* was considered optimal.

From Figure 5 it is obvious that the fitting of the experimental data points is good for θ_3, which is the refined parameter vector from the parameter estimation solution at $k = 3$. The most pronounced improvement in the figure is the fitting of uridine profiles (A) and the recycle line data from using θ_0 to θ_3.

Table 2. Updates of u_k and Termination Criteria

Control variable/ termination criteria	u_0	u_1	u_2^*	u_3
Step time, t_S (min)	2.624	2.677	2.713	2.700
Zone 1 flow rate ratio, m^1	2.870	3.019	3.120	2.997
Zone 2 flow rate ratio, m^2	0.7716	0.9456	0.9156	0.9121
Zone 3 flow rate ratio, m^3	2.808	2.825	2.787	2.799
Zone 4 flow rate ratio, m^4	0.6715	0.7954	0.06578	0.7705
Purity_A^r, %	92.8	94.7	97.8	–
Purity_B^e, %	89.6	98.3	96.2	–
$\left\lvert\frac{\phi_{\text{SMB}}(u_k) - \phi_{\text{SMB}}(u_{k+1})}{\phi_{\text{SMB}}(u_k)}\right\rvert$	0.095	0.017	0.039	–

The simulated concentration profiles have discontinuities at those time points where the next operating conditions are initialized. This discontinuity is also observed in the experiment by using an empty container to collect the extract and raffinate products at the moment the operating conditions are switched. For the recycle line a different sampling strategy was used. The recycle line was not collected in a cumulative way during the experiment. Instead it was sampled once by collecting the average concentration over a step. This was done assuming that after a sufficient number of cycles the cumulative concentration measurement equals the average concentration measurement over a step. This single sample for the recycle line was included in the parameter estimation.

Compared to the change in the Henry's constants there was a significant change in the values of the mass-transfer coefficients from θ_0 to θ_3. This is because the mass-transfer coefficients are less sensitive parameters in the SMB model, and their confidence intervals are large, as discussed later. From u_0 to u_2^*, the operating conditions were varied around the optimal operating conditions, and yet the parameter estimates for θ_1 and θ_3 remained within reasonable ranges.

The optimal operating conditions for each SMB experiment and the final optimization are displayed in Figure 6 in the m^2–m^3 and m^4–m^1 planes to illustrate how the optimal operating conditions evolved as the parameters were refined

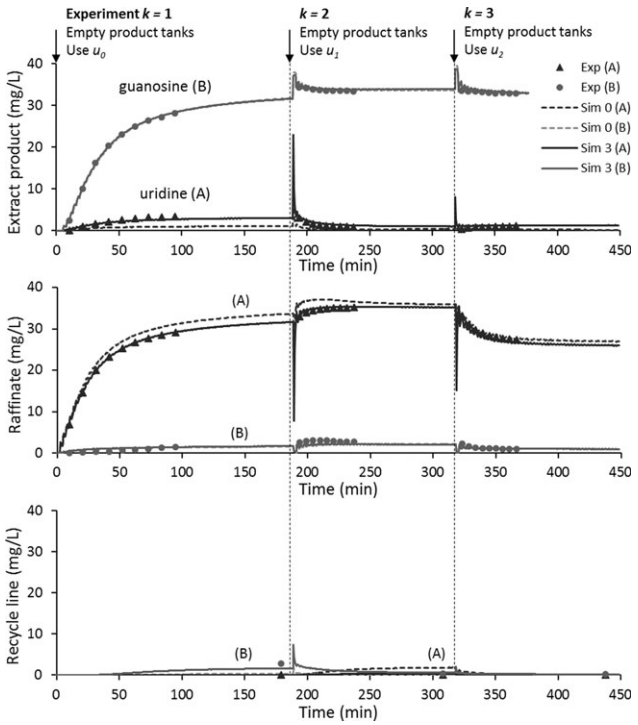

Figure 5. Cumulative concentration data for extract, raffinate and recycle lines from $k = 0$ to $k = 2$ and the parameter estimation fitting.

The dotted lines are the simulated profiles (Sim 0) using θ_0 and the solid lines are the simulated profiles (Sim 3) using θ_3. The operating conditions were switched at the indicated time points and the product containers were emptied to restart the cumulative concentration profiles.

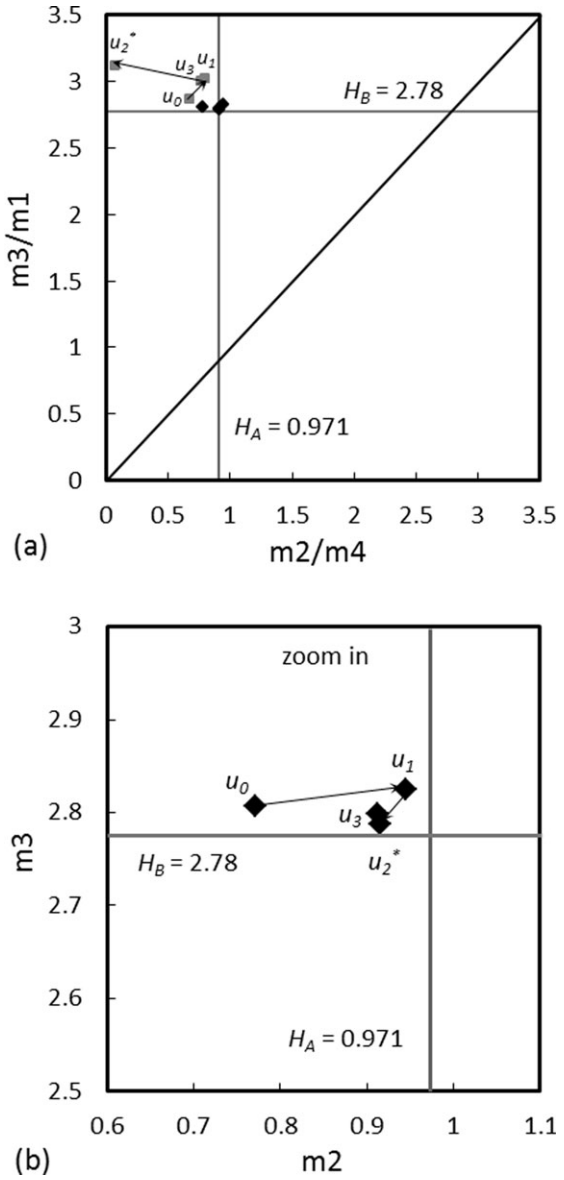

Figure 6. (a) Operating conditions u_0 through u_3 are labeled on the m^2-m^3 (diamonds) and m^4-m^1 (squares) planes with H_A^3 and H_B^3 as boundaries of the triangle region. (b) Zoom in on the m^2-m^3 values for u_0 through u_3.

Note that u_3 was not implemented because the algorithm was terminated at the optimal u_2^*.

at each iteration of the PC algorithm. The boundaries of the triangle region are the values of H_A and H_B in θ_3. In general, the changes in operating conditions for each experiment illustrate the move toward improved product purities from the initial operating condition with poorly estimated parameters. The change from u_1 to u_2 in the m^2-m^3 plane was because the extract product was too pure in $k = 2$, and the raffinate product needed to be further purified. The m^4-m^1 values of a given optimal solution are usually not unique because the desorbent consumption was not included in the objective function. In u_3 the value of m_4 went back to around the same value as in u_1.

Figure 7 shows the improvement of model parameters from $k = 0$ to $k = 1$. The most pronounced improvement in the fitting of the experimental data is in the uridine (A) cumulative concentration profiles. The model mismatch is clear in the uridine profiles and recycle line data using θ_0, hence the need for the correction step. The optimization constraints on product purities were both 96%, yet the measured purities were 89.6% for extract and 92.9% for raffinate, and this mismatch was due to the initial estimation of the model parameters from batch experiments and the existence of dead volumes in the SMB unit. The poor product purities were corrected in the next SMB experiment at $k = 1$ as shown in Table 2.

It should be noted from Figure 7 that the simulated profiles exhibit oscillations at the beginning of this experiment. This is not due to numerical instability of the solver, but as as a result of product concentration profiles within a step. The product concentrations that enter the extract and raffinate tanks have decreasing and increasing patterns, respectively, during a step. These patterns are observed distinctly at the beginning of this experiment where the cumulative amounts of the components in the tanks are still small.

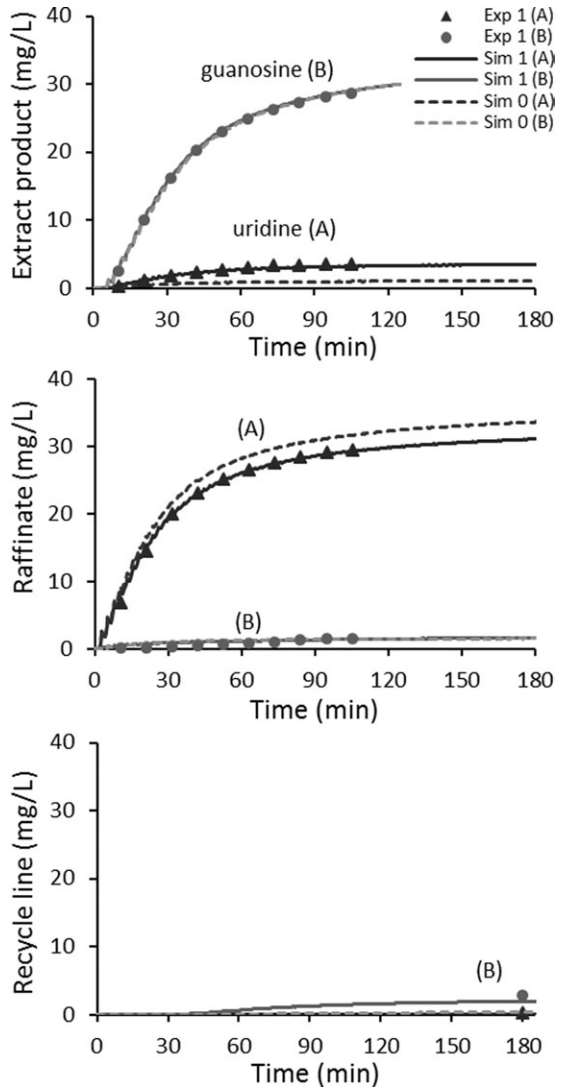

Figure 7. Cumulative concentration data for extract, raffinate, and recycle lines and the parameter estimation fitting.

The dotted lines are the simulation (Sim 0) using θ_0 and the solid lines are the simulation (Sim 1) using θ_1.

The parameter estimation problem (15)–(16) was described previously and the refined model parameters are shown in Table 1. The overall column porosity was kept constant at the initial measured value of 0.820. The following lower and upper bounds were employed in our parameter estimation problem

$$2/3H_{i,0} \leq H_i \leq 3/2H_{i,0}$$

where $H_{i,0}$ is the value of the Henry's constant for component i determined by batch experiments, and

$$\varepsilon_k \leq k_i \leq 1/\varepsilon_k$$

where ε_k is a small positive constant. This constant was selected to be 0.01 based on the results of some sensitivity analysis of the mass-transfer coefficients in the SMB model for this system. It was observed that if the value of k_i was too large then the SMB model produced concentration profiles that were nearly identical and the sensitivity of k_i was lost due to numerical inaccuracy. This happens when the chromatographic columns have a large number of theoretical plates. We confirm that none of these bounds are active at the optimal solutions of all iterations.

Some important observations of the changes in parameter values from θ_0 to θ_1 should be noted. As expected, the Henry's constants in θ_1 were increased from θ_0 by the parameter estimation due to the effect of dead volumes in the SMB unit. This increase is caused by an increase in the apparent retention times of the components in each column because they are further held-up in the dead volumes. In addition, the startup dynamics of the SMB process expose the effect of mass transfer in the SMB model. For example, if mass transfer is fast, then the SMB system reaches CSS sooner. The initial mass-transfer coefficients, which were overestimated in the batch experiment, were corrected by parameter estimation. From Figure 7, it is seen that k_B was decreased to fit the guanosine contamination in the recycle line. Likewise, k_A was decreased to fit the uridine contamination in the extract product.

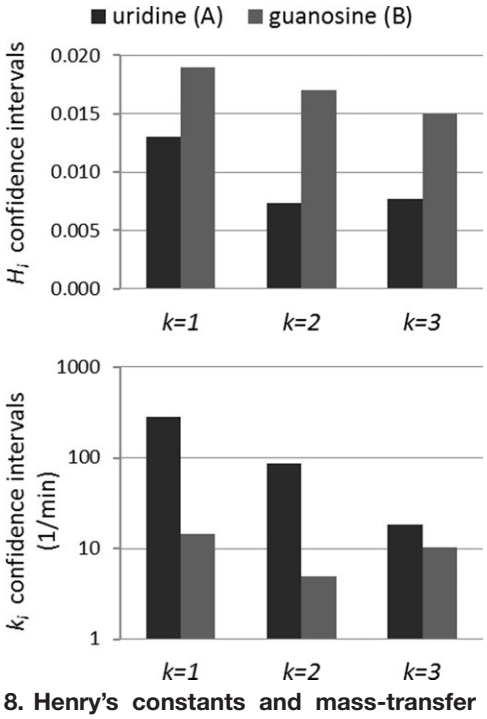

Figure 8. Henry's constants and mass-transfer coefficients 95% confidence intervals for each parameter estimation result from θ_1 through θ_3.

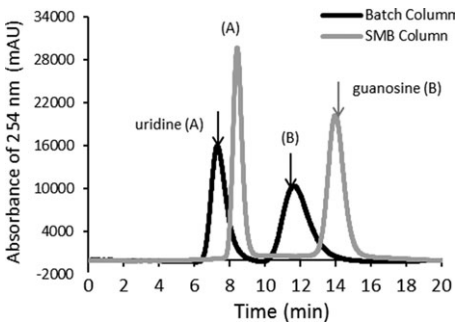

Figure 9. Comparison of chromatograms for the column used in batch experiments and one of the SMB columns.

$F = 3$ mL min^{-1}, $c_{f,A} = c_{f,B} = 50$ mg L^{-1}, injection volume 30 μL, temperature 40°C. The uridine and guanosine peaks are labeled for each chromatogram.

Confidence intervals of parameter estimates

To confirm the reliability of the optimal parameter set, the confidence intervals at 95% statistical confidence were analyzed. In Figure 8 the computed confidence intervals for the Henry's constants, H_i and mass transfer coefficients, k_i are shown at each iteration of the parameter estimation. These statistics were calculated by the parameter estimation routine in gPROMS, and these values depend on the specification of the variance model for experimental measurements discussed in section Step 4 on parameter estimation.

In general, the confidence intervals decreased from one parameter estimation result to the next. The values of the confidence intervals for H_A and H_B were tight relative to the parameter values of 0.971 and 2.80, respectively, and slight improvement was observed. Compared to the Henry's constants, the values of the confidence intervals for k_A and k_B were not tight relative to the parameter values of 52 and 81, respectively. Yet the confidence intervals for k_A and k_B improved significantly from $k = 1$ to $k = 3$. We believe the larger confidence intervals for the mass-transfer coefficients was because of significant variances in the measurements of concentration data, various flow rates in the adsorption zones, and unknown mixing behaviors in the column connections and the main rotary valve.

Robustness of proposed algorithm

We also demonstrate the robustness of the PC algorithm for poor initial model parameters. The system for this case study was 50 mg L^{-1} uridine and 50 mg L^{-1} guanosine dissolved in 95% water 5% methanol. An HPLC column was used to perform batch experiments which had significantly

Table 3. Refinement of θ_0 by Parameter Estimation

Parameter	θ_0	θ_1	θ_{ref}
H_A	1.41	2.91	2.11
H_B	4.96	7.17	6.63
k_A, min^{-1}	20.5	58.1	76.2
k_B, min^{-1}	23.8	3.80	77.3

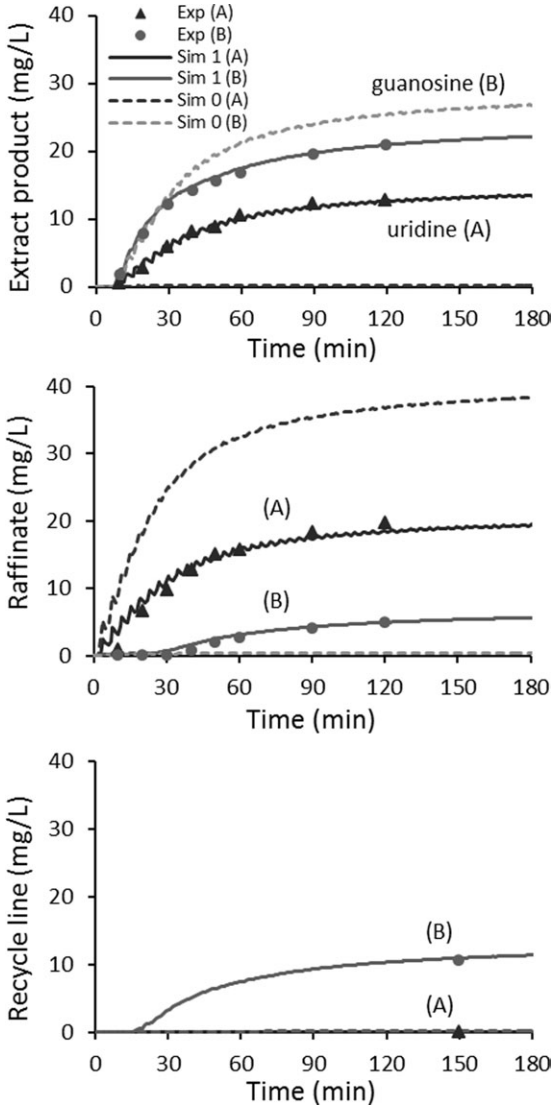

Figure 10. Cumulative concentration data for extract, raffinate, and recycle lines and the parameter estimation fitting.

The dotted lines are the simulation (Sim 0) using θ_0 and the solid lines are the simulation (Sim 1) using θ_1.

different separation performance from the SMB columns used in the experiment. This case study can be considered as a simulation of scale-up where the column packing is inconsistent in a large-scale system, or the lot-to-lot reproducibility of adsorbent is poor. In Figure 9 there is a comparison between the performance of both the ''Batch Column'' and an ''SMB Column.'' The chromatograms are each of 30 μL injections of the feed mixture of uridine and guanosine on the columns with different performance.

The overall porosity of the columns was calculated to be $\varepsilon = 0.806$ by measuring the retention time of uracil. The initial model parameters, θ_0 were calculated by moment analysis of the Batch Column chromatogram. The same model parameters were also calculated by moment analysis of the SMB Column chromatogram for comparison and these are referred to as θ_{ref}. The initial parameter set was refined by parameter estimation after an SMB experiment to obtain θ_1. The initial parameter set, refined parameters from an SMB experiment, and the reference model parameters are shown in Table 3. Note the significant change in the Henry's constants from θ_0 to θ_1; over 100% in H_A and 44% in H_B. Also, the values of the Henry's constants in θ_1 are approaching those in θ_{ref}, but they are increased because of the hold-up in the SMB dead volumes.

Table 4. Update of u_0 After Parameter Estimation and Experimental Purities

Control variable	u_0	u_1
t_S, min	3.843	5.952
m^1	5.930	11.46
m^2	1.636	3.073
m^3	4.228	5.022
m^4	0.9993	2.634
Purity_A^r, %	75.6	99.9
Purity_B^e, %	62.0	99.9

The SMB experimental data and parameter estimation fitting are displayed in Figure 10. There was significant model mismatch observed in the prediction using θ_0 in both uridine (A) and guanosine (B) profiles in all the sampling lines. The expected purities from the model-based optimization were both 99%, but we measured 62.0% in extract and 75.6% in raffinate.

The parameter estimation and optimization, as described earlier, were performed once in this case study to show that the model parameters could be refined to fit the experimental data with reasonable parameter values, and that the operating conditions could be updated to move in a direction of improved product purities. The optimal operating conditions were calculated for θ_0 and θ_1 and the results are shown together with SMB experimental purities in Table 4. The change in operating conditions is shown in Figure 11 to illustrate the large step in a single iteration of the PC algorithm. In this single step the product purities were each increased to 99.9%, and the throughput was reduced by about 50%. This means that the PC algorithm takes aggressive steps and converges quickly if the initial model parameter estimates are poor.

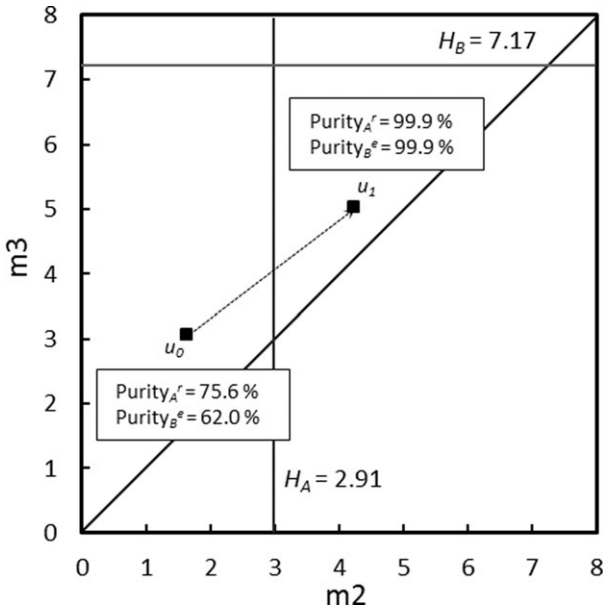

Figure 11. Optimal operating conditions u_0 and u_1 on the m^2-m^3 plane with H_A^1 and H_B^1 as boundaries of the triangle region.

The experimental purities at each operating condition are included.

Conclusions and Future Work

The prediction-correction algorithm for SMB process development has been proposed and tested. It was found to be an efficient algorithm in numerous laboratory experiments with a linear isotherm system, and in the first case study convergence was achieved in only two switches of the operating conditions. In the second case study, the product purities were improved by about 30% in a single step when the initial model parameter estimates were poor. The PC algorithm proceeds in an automatic and sequential manner until it terminates itself so that an SMB expert is not required to manually tune the SMB operating conditions. It should also be noted that this algorithm is designed to function with any choice of the isotherm model. This work demonstrates the algorithm with a linear isotherm, and in the future this algorithm will be verified with experiments on a Langmuir isotherm system. The parameter estimation technique will be tested for the determination of nonlinear isotherm parameters.

Another advantage of obtaining SMB model parameters by the PC algorithm is that we obtain the optimal CSS operating conditions and more reliable parameters that can predict the transient SMB behavior during startup or shutdown. In the near future, we will verify optimal startup and shutdown strategies for SMB as discussed in Li et al.[18] for both linear and Langmuir isotherm systems. Finally, it should be noted that more advanced NLP solvers may improve the computational efficiency.[14]

Acknowledgments

The financial support by Semba Biosciences is gratefully acknowledged. The authors acknowledge the technical support from Daiso Co., YMC Ltd., and Asahi-Kasei Technikrom. The authors specially thank Charlotte Sloan and Joshua Nagy for their aid in experimental work.

Literature Cited

1. Ruthven DM, Ching CB. Counter-current and simulated counter-current adsorption separation processes. *Chem Eng Sci*. 1989;44: 1011–1038.
2. Schmidt-Traub H. *Preparative Chromatography*.Wienheim:Wiley-VCH, 2005.
3. Guiochon G, Felinger A, Shirazi DG, Katti AM. *Fundamentals of Preparative and Nonlinear Chromatography*. San Diego: Academic Press, 2006.
4. Mazzotti M, Storti G, Morbidelli M. Optimal operation of simulated moving bed units for nonlinear chromatographic separations. *J Chromatogr A*. 1997;769:3–24.
5. Lehoucq S, Verheve D, Wouwer AV, Cavoy E. SMB enantioseparation: process development, modeling, and operating conditions. *AIChE*. 2000;46:247–256.
6. Feist SD, Hasabnis Y, Pynnonen BW, Frank TC. SMB chromatorgaphy design using profile advancement factors, miniplant data, and rate-based process simulation. *AIChE*. 2009;55:2848–2860.
7. Grosfils V, Levrie C, Kinnaert M, Wouwer AV. A systematic approach to SMB processes model identification from batch experiments. *Chem Eng Sci*. 2007;62:3894–3908.
8. Grosfils V, Hanus R, Wouwer AV, Kinnaert M. Parametric uncertainties and influence of the dead volume representation in modelling simulated moving bed separation processes. *J Chromatogr A*. 2010;1217:7359–7371.
9. Küpper A, Wirsching L, Diehl M, Schloder JP, Bock HG, Engell S. Online identification of adsorption isotherm in SMB processes via efficient moving horizon state and parameter estimation. *Comput Chem Eng*. 2010;34:1969–1983.
10. Klatt KU, Hanisch F, Dunnebier G, Engell S. Model-based optimization and control of chromatographic processes. *Comput Chem Eng*. 2000;24:1119–1126.
11. Grossmann C, Erdem G, Morari M, Amanullah M, Mazzotti M, Morbidelli M. 'Cycle to cycle' optimizing control of simulated moving beds. *AIChE*. 2008;54:194–208.
12. Biegler LT, Grossmann IE, Westerberg AW. A note on approximation techniques used for process optimization. *Comput Chem Eng*. 1985;9:201–206.
13. Migliorini C, Mazzotti M, Morbidelli M. Simulated moving bed units with extra-column dead volume. *AIChE*. 1999;45:1411–1421.
14. Kawajiri Y, Biegler LT. Optimization strategies for simulated moving bed and PowerFeed processes. *AIChE*. 2006;52:1343–1350.
15. Schiesser WE.*The Numerical Method of Lines: Integration of Partial Differential Equation*.San Diego:Academic Press, 1991.
16. Nilchan S, Pantelides CC. On the optimization of periodic adsorption processes. *Adsorption*. 1998;4:113–147.
17. *Model Validation Guide*. Process Systems Enterprise Ltd. 2011. Available at: www.psenterprise.com.
18. Li S, Kawajiri Y, Raisch J, Seidel-Morgenstern A. Optimization of startup and shutdown operation of simulated moving bed chormatographic processes. *J Chromatogr A*. 2011;1218:3876–3889.

Manuscript received Dec. 23, 2011, and revision received Apr. 6, 2012.